Limbless undulatory propulsion on land

Z. V. Guo* and L. Mahadevan*†‡

*School of Engineering and Applied Sciences and †Department of Organismic and Evolutionary Biology, Harvard University, Cambridge, MA 02138

Edited by George C. Papanicolaou, Stanford University, Stanford, CA, and approved November 30, 2007 (received for review June 12, 2007)

We analyze the lateral undulatory motion of a natural or artificial snake or other slender organism that ''swims'' on land by propagating retrograde flexural waves. The governing equations for the planar lateral undulation of a thin filament that interacts frictionally with its environment lead to an incomplete system. Closures accounting for the forces generated by the internal muscles and the interaction of the filament with its environment lead to a nonlinear boundary value problem, which we solve using a combination of analytical and numerical methods. We find that the primary determinant of the shape of the organism is its interaction with the external environment, whereas the speed of the organism is determined primarily by the internal muscular forces, consistent with prior qualitative observations. Our model also allows us to pose and solve a variety of optimization problems such as those associated with maximum speed and mechanical efficiency, thus defining the performance envelope of this mode of locomotion.

undulatory locomotion | optimization | snake | worm

Slender organisms such as sperms, worms, snakes, and eels propel themselves through a fluid using undulatory waves of flexure that propagate along their body (1). However, undulatory propulsion is not limited to movements through a liquid. Indeed, the side-to-side slithering of snakes, worms, and other elongated organisms that "swim" on land by lateral undulation has piqued the curiosity and interest of humans since biblical times (2).§ It is only in the last century that we have begun to understand this unusual (and seemingly inefficient) mode of locomotion (3). These studies continue into the present, as zoologists try to decipher the neural and physiological bases for the generation of rhythmic patterns of muscular contraction (4, 5) and engineers build and analyze hyper-redundant robotic machines inspired by these organisms (6, 7). From a mechanistic perspective, lateral undulatory locomotion on land has its genesis in the interaction between retrograde flexural waves propagating along the slender body and anisotropic frictional contact with a solid environment.¶ Although this has been known qualitatively for a long time (1, 3, 8, 9), a number of questions remain. In particular, understanding the coupling of the endogenous dynamics of muscular force generation to the exogenous dynamics of the interaction of the organism with its external environment to determine the gait and velocity remains an open question. Furthermore, the important aspects of locomotion associated with gait selection in the presence of sensorimotor feedback are not addressed. Lateral undulatory locomotion on land allows us to approach both these basic questions directly in the context of a relatively simple and realistic model for the exogenous dynamics, allowing the organism's gait, defined here as the periodic shape of the organism, its velocity, and the reactive forces on it to be determined simultaneously. In addition, the simplicity of the model allows us to explore the limits imposed by physics and physiology on movement. Our work thus complements that of biologists who study the anatomical basis, the physiology and performance of limbless undulation on land, as well as that of the robotics community who focus on motion analysis and planning from a control-theoretic perspective.

At first glance, motion by lateral undulation seems paradoxical; the animal glides forward continuously at a constant velocity, tangential to itself everywhere, despite the fact that the only forces in that direction are due to friction, which constantly retards this motion. The resolution of this apparent paradox is clear: propulsion arises due to the in-plane lateral forces generated when the organism braces the sides of its body against the medium or substrate in the presence of an anisotropy of resistance to lateral and longitudinal motion of the slender, curved body (1, 8). A wave of flexure that is fixed in the laboratory frame leads to alternating sideways thrust, which then lead to forward (or backward) movement as shown schematically in Fig. 1*a*. Locomotion, which is achieved through the appropriate coupling of endogenous dynamics to exogenous dynamics, involves four components: (*i*) the endogenous dynamics of force production by muscle, (*ii*) the exogenous dynamics due to the interaction of the organism with its environment, (*iii*) the consideration of linear and angular momentum balance in the body–environment system, and finally (*iv*) the proprioceptive feedback that involves sensorimotor coupling as the organism responds to the forces on and in it. Here we will focus on the first three components by considering the steady lateral undulatory movements of a snake or similar organism on a solid substrate to determine its shape and speed.

Formulation

Equations of Motion. Because snakes are long slender limbless vertebrates, we model one as an inextensible, unshearable filament of length L and circular cross-section (radius R), lying on a plane whose normal is along $\mathbf{z}$, with arc-length $s \in [0, L]$ parameterizing each cross-section along the snake. We denote the position vector of any cross-section of the filament as $\mathbf{r}(s, t)$, so that the tangent to its center line $\mathbf{t}(s, t) = \mathbf{r}_s(s, t)$ makes an angle $\theta(s, t)$ with the x direction (Fig. 1 *a* and *b*). Conservation of linear and angular momentum leads to the equations of motion (10)

$$\mathbf{F}_s + \mathbf{f} = \rho \mathbf{r}_{tt},\ M_s \mathbf{z} + \mathbf{t} \times \mathbf{F} = \rho_0 I \theta_{tt} \mathbf{z}. \qquad [1]$$

Here $(.)_a = \partial(.)/\partial a$, $\mathbf{F}(s, t)$ is the internal force resultant, $M(s, t)\mathbf{z}$ is the internal moment resultant, $\mathbf{f}(s, t)$ is the external force per unit length at each cross-section, ρ_0 is the mass density, $\rho = \rho_0 \pi R^2$ is the mass per unit length, and $I = \pi R^4/4$ is the second moment of the cross section. The kinematic conditions that determine the location of the snake are given by

$$x_s = \cos\theta,\ y_s = \sin\theta,\ \theta_s = \kappa, \qquad [2]$$

where κ is the curvature of the centerline. These conditions impose the constraint of inextensibility naturally. We observe that Eqs. **1** and **2** are valid in a Lagrangian frame that follows each material cross-section along the organism.

Author contributions: Z.V.G. and L.M. designed research, performed research, contributed new reagents/analytic tools, analyzed data, and wrote the paper.

The authors declare no conflict of interest.

This article is a PNAS Direct Submission.

‡To whom correspondence should be addressed. E-mail: lm@seas.harvard.edu.

§Snakes can also move by side-winding, slide-pushing, and stick-slipping (1), but we will not address these different gaits here.

¶The posteriorly oriented scales allow the snake to slip forward more easily than backwards, and further prevent the snake from sliding laterally.

This article contains supporting information online at www.pnas.org/cgi/content/full/0705442105/DCI.

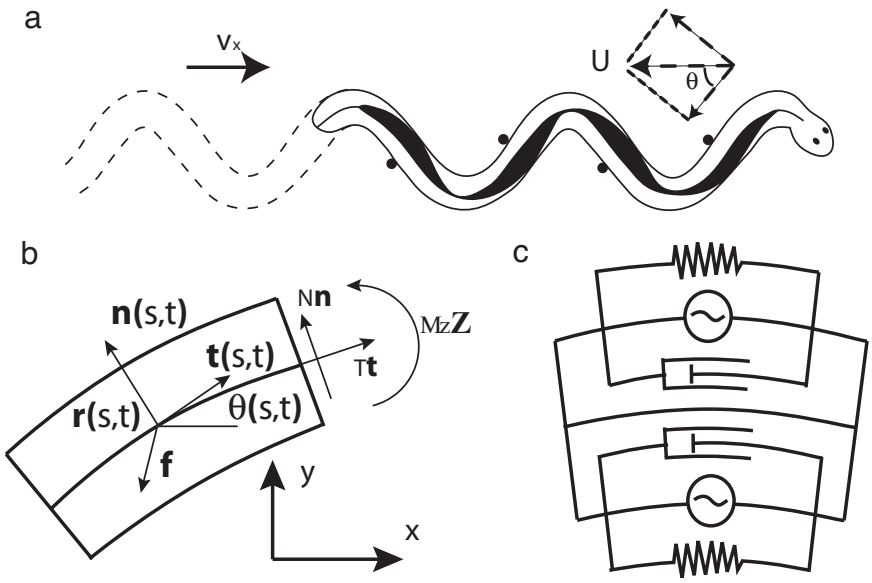

Fig. 1. The model. (*a*) A schematic view of lateral undulation (after ref. 1). The snake is moving at $+x$ direction with a velocity v_x. Solid dots indicate the location of inflection points. The shaded areas qualitatively describe the pattern and amplitude of muscle activity (4, 5). The dotted lines show the track left behind. For undulations without lateral slip, the flexural waves are stationary relative to the ground, and thus the pattern of muscle activity is stationary relative to the lab frame. For undulations with lateral slip, the dashed arrows show the slip velocity in the lab frame *U* and its components along the tangent and normal. (*b*) A small segment of the organism shows the internal forces and moments at a cross-section. (*c*) A visco-elastic model of the same segment contains three parallel elements, a passive elastic element (spring), a passive viscous element (dashpot), and an active muscular element.

For such a filament moving along its own tangent, $\mathbf{r}_t = v(t)\mathbf{t}$, where $v(t)$ is the speed of any (all) point along the filament. Using the identity $(.)_t = v\partial(.)/\partial s$, $\mathbf{r}_{tt} = v_t\mathbf{t} + \kappa v^2\,\mathbf{n}$, where $\mathbf{n}(s, t)$ is the normal to the centerline of the filament (Fig. 1*b*). Decomposing the internal and external forces along the tangent and normal, we write $\mathbf{F} = T\mathbf{t} + N\mathbf{n}$ and $\mathbf{f} = -p\mathbf{n} - (\mu_p|p| + \mu_w\rho g)\mathbf{t}$, where $T(s, t)$ is the tension, $N(s, t)$ is the transverse shear force, $p(s, t)$ is the normal force per unit length of the filament due to its lateral interaction with the substrate, μ_p is the lateral friction coefficient associated with sliding tangentially against the lateral protuberances, and μ_w is the longitudinal friction coefficient associated with sliding on the substrate. Using $\theta_{tt} = v^2\,\kappa_s + v_t\kappa$, Eq. **1** may be rewritten, in component form, as

$$T_s - \kappa N - \mu_p|p| - \mu_w\rho g = \rho v_t \qquad [3]$$

$$N_s + \kappa T - p = \rho v^2\kappa \qquad [4]$$

$$M_s + N = \rho_0 I(v^2\kappa_s + v_t\kappa). \qquad [5]$$

We observe that Eqs. **2–5** form a set of six equations for the nine unknowns $x, y, \theta, \kappa, v, T, N, M, p$ that include the shape of the snake, the internal forces and moments in it, the external normal force on it, and the velocity of motion. To complete the formulation, we need to supplement Eqs. **2–5** with some additional closure relations for the internal moment M and the external normal force p (a Lagrange multiplier that enforces the condition of no transverse slip) and supply some boundary and initial conditions. Focusing on steady lateral undulations ($v_t = 0$) without lateral slip implies that the above equations are also valid in the lab frame, because Eqs. **2–5** are Galilean invariant (under the transformation $s' = s - vt$). From hereon, we will consider only the case of steady undulation in the lab frame.

Closure and Scaling. The internal moment $M(s, t)$ at any cross-section consists of a passive component with its origins in the response of tissue that resists deformation, and an active component with its origins in muscular contraction. A simple model for the passive response of tissue is afforded by the linear Voigt model for viscoelasticity (11), which states that the uniaxial stress in bulk tissue $\sigma = E\,\varepsilon + \eta\dot{\varepsilon}$, with ε and $\dot{\varepsilon}$ being the strain and strain rate in the tissue, E being the Young's modulus, and η being the viscosity of the tissue (12, 13) (Fig. 1*c*). For the inextensible bending of slender body, this implies that the passive moment $M_p = M_e + M_v$, where M_e and M_v are the elastic and viscous moments, and $M_e = EI\kappa$, $M_v = \eta I v\kappa_t = \eta I v\kappa_s$. During lateral undulatory locomotion, muscles on either side of the body are activated alternatively (4), become active at the point of maximal convex flexion, and cease activity at the point of maximal concave flexion. This leads to an alternating active flexural moment generated by the muscles which connect the vertebrae and skin of the snake; the pattern and amplitude of muscle activity are qualitatively described by the shaded area shown in Fig. 1*a*. In general, there is a time delay between muscle activation and the development of contractile force (≈ 0.1 s, ref. 14); however, since this time is much smaller than the period of muscle contraction (≈ 1 s, ref. 5), we will neglect the effects of this delay here. The simplest form of the active moment that is consistent with this periodic pattern of muscle activity is $M_a = m_a \sin(2\pi s/l)$, $s \in [0, l]$, where l is the arc-length within one period and m_a is the amplitude of the active moment. Then, the total internal moment, which is the sum of the passive and active moments, is given by

$$M = m_a \sin(2\pi s/l) + EI\kappa + \eta I v\kappa_s. \qquad [6]$$

We also need a relation for the forces associated with the interaction of the snake with the external environment, characterized by the normal force per unit length p. We note that $p(s)$ should (*i*) be periodic, except near the ends; (*ii*) switch signs at the locations of the maximally curved regions because the lateral force in the neighborhood of these points does not contribute to active propulsion; and (*iii*) have a maximum in between the maximally curved regions, which is consistent with observations. To go further, we consider three different forms of p that satisfy the above conditions; (*I*) $p = C(\delta(s - l/4) - \delta(s - 3l/4))$, i.e., it is localized at the inflection points of the (unknown) path, corresponding to the situation when the snake pushes against an array of pegs (1). (*II*) $p = C \sin(2\pi s/l)$,

i.e., it is proportional to the active moment, because a larger active moment results in a large normal force. (*III*) $p = C \sin\theta$, i.e., it is determined by the local shape of the snake. To understand this last limit, we first consider the creeping motion of a worm or snake in a viscous liquid. Then the viscous force on the body is proportional to its relative speed to the medium (15), so that the lateral force per unit length $p(s) = C_\perp U \sin\theta$, where $C_\perp$ is the drag coefficient along the normal $\mathbf{n}(s, t)$, U is the slip velocity relative to the medium, and $U \sin\theta$ is the lateral slip velocity (Fig. 1*a*). For undulations without lateral slip [see supporting information (SI) *Appendix* for the case of undulations with lateral slip], we consider the limiting process where $C_\perp \to \infty$, $U \to 0$, but $C_\perp U = C =$ constant, which leads to the above formula for p. For all three forms of p, $C > 0$ has the dimensions of force per unit length, and is a phenomenological characterization of the organism's interaction with its environment. These closure relations for M, p do not account for sensorimotor feedback or proprioception, but do allow us to formulate a series of problems for gait selection as a function of the endogenous and exogenous dynamics. In the following, we will use

$$p = C\sin\theta \qquad [7]$$

for ease of analysis, but our calculations with the other forms (see *SI Appendix*) yields qualitatively similar results for the factors that determine the gait and velocity of the snake.

For steady undulations, $v_t = 0$. Then, substituting for the shear force N from Eq. **5**, the torque M from Eq. **6** and the normal force per unit length p from Eq. **7** into Eqs. **3** and **4** leads to the system

$$\begin{aligned} T_s &= \mu_w \rho g + \mu_p C|\sin\theta| - \frac{2\pi}{l} m_a \cos\left(\frac{2\pi s}{l}\right)\kappa \\ &\quad - (E - \rho_0 v^2) I \kappa \kappa_s - \eta I v \kappa \kappa_{ss} \\ C\sin\theta &= \left(\frac{2\pi}{l}\right)^2 m_a \sin\left(\frac{2\pi s}{l}\right) + \kappa(T - \rho v^2) \\ &\quad - (E - \rho_0 v^2) I \kappa_{ss} - \eta I v \kappa_{sss} \end{aligned} \qquad [8]$$

for the variables $\theta(s)$, $T(s)$, with s the coordinate in the traveling wave frame. In terms of the dimensionless variables $\bar{s} = s/l$, $\bar{x} = x/l$, $\bar{y} = y/l$, $\bar{\kappa} = \kappa l$, $\bar{T} = (T - \rho v^2)/\rho g l$ we can rewrite Eqs. **8** and **2**, on dropping the bars, as

$$\begin{aligned} T_s &= \mu_w + \mu_p \mathrm{Pr}|\sin\theta| - \mathrm{Mo}\,\frac{\cos(2\pi s)\kappa}{2\pi} - \mathrm{Be}\kappa_s\kappa - \mathrm{Vi}\kappa_{ss}\kappa, \\ 0 &= -\mathrm{Pr}\sin\theta + \mathrm{Mo}\sin(2\pi s) + \kappa T - \mathrm{Be}\kappa_{ss} - \mathrm{Vi}\kappa_{sss}, \\ x_s &= \cos\theta, y_s = \sin\theta, \theta_s = \kappa, s \in [0,\ 1]\ . \end{aligned} \qquad [9]$$

Here, the dimensionless parameters μ_w and μ_p are the longitudinal and lateral friction coefficients; $\mathrm{Mo} = 4\pi^2 m_a/\rho g l^2$ is the dimensionless amplitude of the active moment, $\mathrm{Pr} = C/\rho g$ is the dimensionless lateral resistive force, and $\mathrm{Be} = (E - \rho_0 v^2) I/\rho g l^3$ and $\mathrm{Vi} = \eta I v/\rho g l^4$ are the dimensionless passive elastic and viscous bending stiffnesses of the slender organism. These dimensionless parameters fall into two categories: μ_w, μ_p, Pr, which characterize the exogenous dynamics of the system, and Mo, Be, Vi, which characterize the endogenous dynamics of the system. For snakes moving on a variety of surfaces, $\mu_w \approx \mu_p \approx 0.2$, $\mathrm{Pr} \in [0.1, 100]$, $\mathrm{Mo} \in [0, 200]$, $\mathrm{Be} \in 4[10^{-4}, 0.1]$, and $\mathrm{Vi} \in 4[10^{-5}, 0.01]$ (see *SI Appendix*). To complete the formulation of the boundary value problem, we must specify some boundary conditions. To eliminate rigid displacements and rotations, we let $x(0) = y(0) = \theta(0) = 0$. For long snakes, ignoring end effects (see *SI Appendix*), we look for periodic solutions so that

$$x|_0 = y|_0 = y|_1 = \theta|_0 = \theta|_1 = 0, T|_0 = T|_1, \kappa|_0 = \kappa|_1, \kappa_s|_0 = \kappa_s|_1. \qquad [10]$$

Periodic solutions also require $\kappa_{ss}|_0 = \kappa_{ss}|_1$; we note that this condition follows by integrating the second equation in Eq. **9** subject to Eq. **10**.

The nonlinear system (Eqs. **9** and **10**) forms a seventh-order system of ODEs with eight boundary conditions for the unknown shape ($x, y, \theta, \kappa, \kappa_s, \kappa_{ss}$), the tension T, the speed v and the arc-length within a period l. This freedom implies that we may, for example, arbitrarily choose the speed v and arc-length within a period l to account for the fact that the snake can vary its velocity and wavelength during undulation (this fixes Be and Vi for a given organism) and determine the amplitude of the active moment $\mathrm{Mo} = \mathrm{Mo}(\mu_w, \mu_p, \mathrm{Pr}, \mathrm{Be}, \mathrm{Vi})$. Alternately, we may choose Mo and determine v and the other parameters, thus relating the endogenous and exogenous dynamics to the shape and speed of the snake. If, in addition, there are physiological constraints such as limits on muscular performance, speed of contraction, maximum force, etc., some of the parameters are related to each other; this would then lead to further limitations on the locomotory performance envelope of the organism.

Steady Undulation

We now consider the effects of the exogenous and endogenous dynamics on steady movement with the aim of determining the shape and speed of the organism as a function of its active and passive properties as well as its interaction with its environment. To simplify matters, we will use $\mu_w = \mu_p = 0.2$ for the friction coefficients in all the numerical calculations.

For small-amplitude, long wavelength undulations, we may write $\theta = \theta_0 \sin(2\pi s)$ with $\theta_0 \ll 1$. Substituting this expression into Eq. **9,** after some rearrangement, we find that (see *SI Appendix*)

$$-T_s + \mu_w - \frac{\mathrm{Mo}_0\theta_0(1 + \cos(4\pi s))}{2} - \mathrm{Be}\kappa_s\kappa + \mu_p \mathrm{Pr}\theta_0|\sin(2\pi s)| = O(\theta_0^2) \qquad [11]$$

$$(\mathrm{Mo}_0 - \mathrm{Pr}\theta_0)\sin(2\pi s) = O(\theta_0^2) \qquad [12]$$

$$x_s = 1 + O(\theta_0^2), y_s = \theta + O(\theta_0^3), \qquad [13]$$

where

$$\mathrm{Mo}_0 = \mathrm{Mo} - (2\pi)^4 \theta_0 \mathrm{Vi}. \qquad [14]$$

To leading order, Eq. **12** yields

$$\mathrm{Mo}_0 = \mathrm{Pr}\theta_0. \qquad [15]$$

Substituting Mo_0 into Eq. **11,** and using the periodicity condition $\int_0^1 T_s\, ds = 0$, we get

$$\frac{\mathrm{Pr}}{2}\theta_0^2 - \frac{2\mu_p \mathrm{Pr}}{\pi}\theta_0 - \mu_w = 0 \qquad [16]$$

with only one positive solution

$$\theta_0 = \frac{2\mu_p}{\pi} + \sqrt{\left(\frac{2\mu_p}{\pi}\right)^2 + \frac{2\mu_w}{\mathrm{Pr}}}. \qquad [17]$$

This allows us to determine the normalized shape of the snake by integrating Eq. **13**, which yields

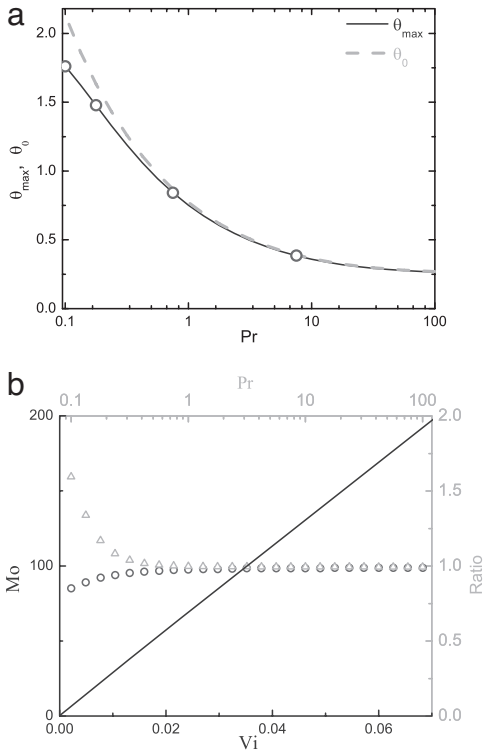

Fig. 2. Comparison of analytical and numerical solutions. (*a*) The maximum tangent angle θ_{max} obtained by numerically solving (Eq. **9**) is well approximated by θ_0, the amplitude of θ obtained from the linearized Eqs. **11**–**13**. Different circles correspond to the values of Pr for the shapes shown in Fig. 3*b*. Here, Be = 0.4, Vi = 0.04, although Be and Vi do not affect the normalized shape of the snake (i.e., θ_{max}) (see Fig. 3*a*). (*b*) The dimensionless active moment Mo, obtained from the numerical solution of Eq. **9**, is a linear function of the dimensionless passive viscosity Vi (left and bottom axis, Pr = 0.1, Be = 0.4). We also fit Mo using $k_1 + k_2$ Vi and plot k_1/Mo_0 (triangles), $k_2/(2\pi)^4\ \theta_0$ (circles) (top and right axis). k_1/Mo_0 and $k_2/(2\pi)^4\ \theta_0$ are ≈1 when Pr > 0.2, which validates Eq. **14**. The scaled elastic bending stiffness Be used here is 0.4, but the exact value does not affect Mo (see text).

$$x = s + O(\theta_0^2), y = \frac{\theta_0}{2\pi}(1 - \cos(2\pi s)) + O(\theta_0^3),\ s \in [0,1]. \qquad [18]$$

To determine the regime of validity of this approximate solution, we solve the complete system (Eqs. **9** and **10**) numerically using the boundary value problem solver *bvp4c* in Matlab. In Fig. 2 *a* and *b* we show the variation of the amplitude θ_0 as a function of Pr for comparison with Eq. **17**, and the relation between Mo and Vi for comparison with Eqs. **14** and **15**. We find that the approximate solution to the linearized equations agrees well with the numerical results even when the normalized shape of the snake is far from a sinusoidal curve.

Exogenous Dynamics. The results of our linearized analysis, summarized in Eqs. **17** and **18**, suggest that the normalized shape of the steadily moving snake depends only on the exogenous parameters: the longitudinal and lateral friction coefficients μ_w and μ_p, and the lateral resistive force Pr. Indeed, in Fig. 3*a*, we show that the normalized shapes for various values of the dimensionless passive elastic and viscous resistance Be, Vi collapse into a single curve, i.e. the passive elasticity and viscosity of the snake do not affect the normalized shape of the snake. An immediate implication of this result is that for a given environment, if the arc-length within a period l (and thus the wavelength within a period λ) remains

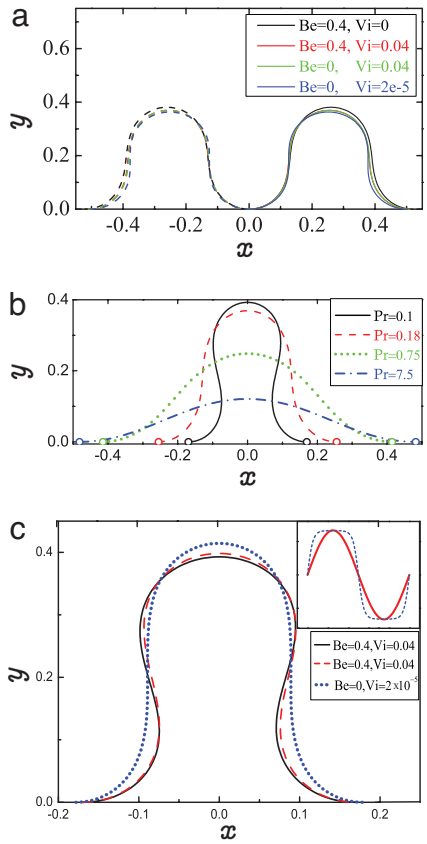

Fig. 3. The effects of exogenous and endogenous dynamics on the normalized shape of a snake. (*a*) The effects of scaled passive elasticity Be and viscosity Vi on the shape of the snake normalized by the arc-length in a period. The solid line shows one period, whereas the dashed line shows the track, which is the same as the solid line, left behind. The observed collapse of all the shapes shows that the passive elasticity and viscosity do not affect the normalized shape. Here, Pr = 0.18. (*b*) The effects of exogenous dynamics, i.e., the substrate resistance Pr, on the normalized shape of the snake; we see that the normalized amplitude is large when Pr is small and small when Pr is large. Here, Be = 0.4, Vi = 0.04. (*c*) The effects of two extreme forms of the active moment on the normalized shape, with $M_{a1} = m_{a1}\sin(2\pi s)$ (solid), $M_{a2} = m_{2a}\tanh(3\sin(2\pi s))$ (dashed and dotted) (*Inset*). We see that the normalized shape is not strongly affected by the form of the active moment, for a range of values of Be and Vi. Here, Pr = 0.1.

constant, the snake can increase its projected velocity in the direction of motion $v_x = \omega\lambda/2\pi$ by increasing the frequency ω of its flexural waves. This is qualitatively consistent with observations of lateral undulatory motion of limbless lizards and snakes on land (16–19) who increase their velocity by increasing their frequency of bending.

The solution (Eq. **17**) also shows that the amplitude of undulation θ_0 is large when Pr is small, i.e. when the substrate is easily deformable and small when Pr is large (Fig. 2*a*), i.e. when the substrate is not very deformable. When $\mathrm{Pr} >> \mu_w/\mu_p^2$, the frictional drag due to the snake's weight is unimportant and the normalized shape does not change much with Pr; however, when $\mathrm{Pr} \ll \mu_w/\mu_p^2$, the frictional drag due to the snake's weight is important and $\theta_0 \sim 1/\sqrt{\mathrm{Pr}}$. The cross-over occurs when $\mathrm{Pr} \approx \mu_w/\mu_p^2 = 5$. In Fig. 3*b*, we show the normalized shape of a period of the snake $x(s)$, $y(s)$ for various values of Pr obtained by solving the nonlinear system (Eq. **9**). The results are consistent with (Eq. **17**); the normalized shape has a small amplitude when the substrate is not very deformable, and has a large amplitude when the substrate is easily deformable.

Endogenous Dynamics. We now turn to the role of the active moment in determining the gait of the organism. We have seen that the

passive elasticity and viscosity characterized by the parameters Be and Vi do not affect the normalized shape of a snake when the active moment is a simple periodic function. To investigate the effect of the form of the active moment, we consider two extremes: a simple sinusoid $M_{a1} = m_{a1}\sin(2\pi s/l)$ and an approximation to a square wave $M_{a2} = m_{a2}\tanh(3\sin(2\pi s/l))$. In Fig. 3*c*, we show that the normalized shape of the snake for the two forms of the active moment is essentially the same for a range of values of Be, Vi, i.e., it is independent of the detailed distribution of muscular forces along its body.

However, the active moment is clearly important in determining the speed and the energetics of lateral undulatory locomotion, which we will now consider. During steady undulation, the power generated by muscular contraction is balanced by the dissipation due to endogenous and exogenous sources. Substituting Eq. **6** into Eq. **5** and using Eq. **3** yields, after integrating over one period by parts using Eq. **10**, the power balance equation

$$-v\int_0^1 \kappa_s M_a ds = v\int_0^1 (\mu_w \rho g + \mu_p |p| + \eta I v \kappa_s^2) ds. \qquad [19]$$

Here, the left side is the power generated by the active moment, and the right side is the sum of the power dissipated by external frictional forces and the internal (viscous) frictional dissipation. In the small amplitude approximation, with $\theta = \theta_0 \sin(2\pi s)$, the scaled version of Eq. **19** reads $\mathrm{Mo} = 2(\mu_w + 2\mu_p \mathrm{Pr}\theta_0/\pi)\theta_0 + (2\pi)^4\theta_0\,\mathrm{Vi} = \mathrm{Mo}_0 + (2\pi)^4\theta_0\,\mathrm{Vi}$, where the last equality follows from Eq. **16**. We observe that this relation is identical to Eq. **14**, which we can also interpret as an equation for power balance. We see that the dissipation due to the lateral force dominates the contribution due to the weight of the body when $2\mu_p \mathrm{Pr}\theta_0/\pi > \mu_w$, while the dissipation due to internal friction is important when $(2\pi)^4\theta_0^2\mathrm{Vi} > 2\mu_w$. It is worth noting that these approximate results based on an analysis of the linearized equations are valid even when the amplitude is not small (see Fig. 2*b*).

Optimal Undulation

Having characterized lateral undulatory movements in the absence of any optimization criterion-imposed constraints, we now turn to some problems that involve the optimization of lateral undulatory movements that arise naturally; that of maximizing mechanical efficiency, that of minimizing the internal torque, and that of maximizing the velocity of progression. Answering these questions allows us to set the absolute scale of the speed v and arc-length per wave l of the organism, and thus define the performance envelope of this mode of locomotion.

Maximizing Mechanical Efficiency. Our energetic estimates allow us to define a mechanical efficiency of lateral undulatory movement χ as the ratio of the energy required to move an inactive limbless organism in the direction of motion to the energy expended internally and externally due to active lateral undulatory movements, so that

$$\chi = \frac{\int_0^1 \mu_w \rho g \cos\theta ds}{\int_0^1 (\mu_w \rho g + \mu_p |p| + \eta I v \kappa_s^2) ds}, \qquad [20]$$

which, in terms of the scaled variables, may be written as

$$\chi = \frac{\int_0^1 \mu_w \cos\theta ds}{\int_0^1 (\mu_w + \mu_p \mathrm{Pr}|\sin\theta| + \mathrm{Vi}\kappa_s^2) ds}. \qquad [21]$$

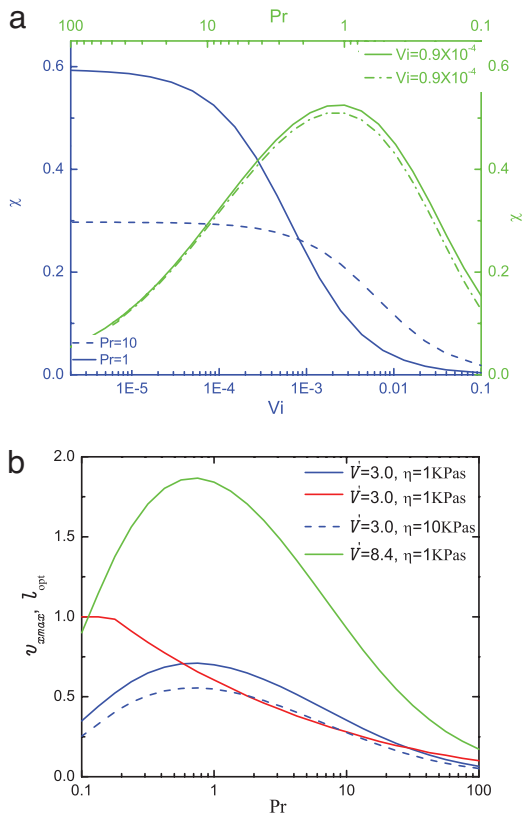

Fig. 4. The energetics and efficiency of lateral undulatory locomotion. (*a*) The mechanical efficiency χ as a function of Pr (top right axes) and Vi (bottom left axes), obtained by solving Eq. **9** numerically (solid line) is well approximated by Eq. **22** (dash-dot line). (*b*) The optimum arclength l_{opt} (red curve) and the maximum projected velocity $v_{x_{max}}$ (rest curves) as a function of Pr. The environment temperatures are 15°C ($V' = 3.0/s$) and 25°C ($V' = 8.4/s$). The maximum of l_{opt} is 1 m, the length of the snake. For all the calculations, $c = 4$, $\delta = 0.2$, and $\mathrm{Be} = 0.4$.

In the small amplitude approximation, with $\theta = \theta_0 \sin(2\pi s)$, we find that

$$\chi \approx \frac{2\mu_w \lambda/l}{(\mu_w + 2\mu_p \mathrm{Pr}\theta_0/\pi + (2\pi)^4\theta_0^2 \mathrm{Vi})} = \frac{2\mu_w \lambda/l}{\mathrm{Mo}\theta_0}, \qquad [22]$$

where θ_0, Mo are given by Eqs. **17** and **14**, respectively. We see that the mechanical efficiency is proportional to the projection of the undulation in the direction of motion λ/l, and is inversely proportional to the active moment Mo. In Fig. 4*a*, we show the variation of the mechanical efficiency χ as a function of Pr and Vi, obtained by solving the complete nonlinear system (Eq. **9**). Again, we see that the analytical approximation (Eq. **22**) is able to capture the dependence of the efficiency on Pr and Vi well. As expected, an increase in Vi reduces the mechanical efficiency. However, Pr affects the mechanical efficiency nonmonotonically, because small values of Pr imply a small projection of the velocity in the direction of movement, i.e. a small λ/l, whereas large values of Pr lead to a large lateral frictional dissipation. By maximizing the mechanical efficiency defined by Eq. **22**, we find the χ reaches its maximum when l reaches its maximum, and is of the order of the organism's body length. This result could help rationalize the observation that there are usually only one or two waves along the body of snakes, worms and other slender undulating organisms.

So far, we have not considered any limitations on the active moment m_a. In extreme conditions when the muscles of the snake are maximally contracted, it pays to minimize the amplitude of the

active moment m_a. When m_a in Eq. **14** is minimized with respect to l for a given υ, we get an expression for the arc-length in a wavelength given by

$$l = 2\pi(\eta I\upsilon/C)^{1/4} = 2\pi R(\pi\eta\upsilon/4C)^{1/4}. \quad [23]$$

We note that this power law makes l relatively insensitive to η, υ, C. Using typical values for a 1-m-long grass snake with $R = 1.25$ cm, $\upsilon = 0.1m/s$, $\eta = 10$ KPas, and $C \sim \rho g \sim 1$ N/m, we find $l_{opt} \approx 0.42m$, which is qualitatively consistent with observations.

Maximizing Velocity. Muscles have their physiological limitations. When skeletal muscle is maximally activated, i.e., it is in a tetanized state, the contractile stress and velocity of the muscle are related by the Hill relation (20)

$$P/P_0 = (1 - V/V_0)/(1 + cV/V_0), \quad [24]$$

where P is the contractile stress in muscle, P_0 is the maximal contractile stress, V is the velocity of muscle contraction, V_0 is the maximum velocity of muscle contraction and c is the Hill parameter characterizing muscle type (see *SI Appendix*). In lateral undulatory locomotion, assuming that the contractile stress P acts over an areal fraction δ of muscle at each cross-section and an effective moment arm R (see Fig. 1*a*), for a simple sinusoidal form of the contractile moment, we may write

$$m_a \sin(2\pi s/l) = P\cdot\pi R^2\delta/2\cdot R, \quad [25]$$

where a factor of 1/2 accounts for the fact that muscles are activated only on one side of the snake at a given instant of time. From Eq. **25**, we see that the contractile stress required to produce the active bending moment reaches its maximum at $s = l/4$. The velocity of contraction V for a steadily moving organism is the strain rate of the muscle times its length l_0, so that

$$V = (R\kappa)_t l_0 = R\kappa_s \upsilon l_0. \quad [26]$$

From Eq. **24**, we see that P is a decreasing function of V, and reaches its minimum at the inflection point $s = l/4$ where V, κ_s reach their maximum (Eq. **26**), so that the muscle there first reaches the limits determined by the Hill relation. In the linearized approximation inherent in Eq. **14**, this allows us to write the scaled form of the Hill relation (Eq. **24**) at $s = 1/4$ in terms of Eqs. **25** and **26** as

$$a_1\frac{1 - a_2\upsilon}{1 + ca_2\upsilon} = \mathrm{Mo}_0 + a_3\upsilon \quad [27]$$

where $a_1 = 2\pi^2\,\delta\,P_0\,R/\rho_0 g l^2$, $a_2 = |\bar{\kappa}_{\bar{s}}|_{1/4}R/V'l^2$, $a_3 = 4\pi^4\theta_0\eta R^2/\rho_0 g l^4$, $V' = V_0/l_0$, and $\bar{\kappa}_{\bar{s}}$ is the dimensionless form of κ_s. This additional physiological constraint implies that when the muscle of the snake is maximally activated, the velocity $\upsilon = \upsilon(l)$, i.e. it is a function of the arc-length l and cannot be chosen independently. This allows us to pose another optimization problem: for a given snake moving in a given environment what is its maximum velocity projected in the direction of motion, $\upsilon_{x_{\max}} = \max(\upsilon\int_0^1 \cos(\theta)\,ds)$? In Fig. 4*b* we use Eq. **27** to determine the maximum projected velocity $v_{x_{max}}$ as a function of Pr. The Hill relation then also allows us to determine the optimum choice of the arc-length in a period l_{opt}, as a function of Pr. We see that $v_{x_{max}}$ peaks for an intermediate value of Pr. To understand this we observe that when Pr is small, the undulations are large and thus the projected velocity is small. When Pr is large, the larger frictional forces cause the organism to have a smaller velocity. This implies that there is an optimal substrate on which the snake moves fastest, which is consistent with quantitative experiments on the speed of garter snakes moving on different substrates (21). This maximum velocity $v_{x_{max}}$ is qualitatively the same over a range of values of areal fraction of muscle at each cross-section δ, and the Hill parameter c. However, $v_{x_{max}}$ is sensitive to changes in V' the maximal muscle contraction velocity which varies with temperature: for example, $v_{x_{max}}$ at 25° C is more than twice larger than that at 15°C (solid green and blue curves) when Pr $\sim$ 1, consistent with observations (22, 23). The Hill relation (Eq. **27**) also allows us to study the effects of size on speed, an aspect that is discussed elsewhere (*SI Appendix*).

Discussion

In this paper, we have tried to dissect the role of the various exogenous and endogenous dynamical variables that characterize these movements in a hitherto unexplored context: undulation on an anisotropic frictional environment that does not allow for transverse slip. Our mathematical model, which leads to a nonlinear boundary value problem, accounts for the role of a passive collective viscoelasticity of the tissue, an active moment subject to certain physiological constraints and a simple frictional law that accounts for the interaction of the slender organism with the environment.

A combination of analysis and numerical simulation of the model yields a number of results which we summarize: the normalized shape of the organism is determined primarily by the interaction of the organism with its external environment, whereas the speed and energetics of locomotion are determined by the internally generated periodic active moment generated by muscle contraction. These results are consistent with prior qualitative experimental observations. In addition, we can define parts of the performance envelope of undulatory propulsion on land by posing and solving some simple optimization problems for the maximization of the efficiency and velocity of the organism. However, our analysis is limited to a consideration of steady movement without proprioceptive feedback, which effect is crucial in understanding how the organism responds to the forces that it senses, so that many questions remain for further study.

1. Gray J (1968) *Animal Locomotion* (Cambridge Univ Press, Cambridge, UK), 2nd Ed.
2. Proverbs, XXX.19. "The way of a serpent on the rock," one of Solomon's riddles.
3. Mossauer W (1932) *Science* 76:583–585.
4. Jayne BC (1988) *J Morphol* 197:159–181.
5. Moon BR, Gans C (1998) *J Exp Biol* 201:2669–2684.
6. Hirose S (1993) *Biologically Inspired Robots: Snake Like Locomotors And Manipulators* (Oxford Univ Press, Oxford).
7. Ostrowski J, Burdick J (1998) *Int J Robotics Res* 17:683–701.
8. Fokker AD (1927) *Physica* 7:65–71.
9. Kuznetsov V, Lugovtsov B, Sher Y (1967) *Arch Rat Mech Anal* 25:367–387.
10. Landau L, Lifshitz EM (1986) *Theory of Elasticity* (Pergamon, New York), 3rd Ed.
11. Fung YC (1981) *Biomechanics: Mechanical Properties of Living Tissues* (Springer, New York).
12. Bowtell G, Williams TL (1991) *Philos Trans R Soc London B* 334:385–390.
13. Cheng J-Y, Pedley TJ, Altringham JD (1998) *Philos Trans R Soc London B* 353:981–997.
14. Hatze H (1977) *Biol Cybernet* 25:103–119.
15. Gray J, Hancock GJ (1955) *J Exp Biol* 32:802–814.
16. Walton M, Jayne BC, Bennett AF (1990) *Science* 249:524–526.
17. Gasc J-P, Gans C (1990) *Copeia* 1990:1055–1067.
18. Gans C, Gasc J-P (1990) *J Zool* 220:517–536.
19. Gasc C, Morgan WK, Allen ES (1992) *Herpetolotica* 48:246–262.
20. McMahon T (1984) *Muscles, Reflexes and Locomotion* (Princeton Univ Press, Princeton).
21. Kelley KC, Arnold SJ, Gladstone J (1997) *Funct Ecol* 11:189–198.
22. Mosauer W (1935) *Copeia* 1:6–9.
23. Finkler MS, Claussen DL (1999) *J Herpetol* 33:62–71.